

# Memantine Attenuates Cognitive and Emotional Dysfunction in Mice with Sepsis-Associated Encephalopathy

XiaoYu Zheng,<sup>#</sup> WenYu Li,<sup>#</sup> Qian Xiang, YanXue Wang, TingYu Qu, Wei Fang, and HongNa Yang\*



Cite This: *ACS Omega* 2023, 8, 40934–40943



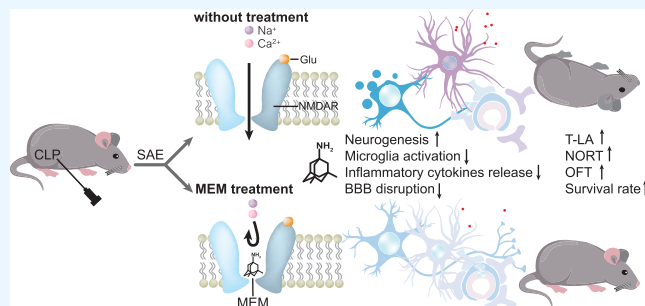
Read Online

ACCESS |

Metrics & More

Article Recommendations

**ABSTRACT:** Sepsis-associated encephalopathy (SAE) is the most common complication of sepsis, with increased morbidity and mortality. To date, there has still been no established pharmacological therapy. Memantine, as an NMDA (*N*-methyl-D-aspartate) receptor antagonist, exhibited neuroprotective effects against cognitive and emotional dysfunction in many disorders. We performed cecal ligation and puncture (CLP) inducing sepsis as the ideal animal model of SAE. CLP-induced septic mice were given a memantine treatment through intragastric administration. The novel object recognition test indicated that memantine significantly improved cognitive dysfunction in septic mice. The open field test revealed that the anxiety-like behaviors and locomotion ability of septic mice were relieved by memantine. The pole test further confirmed the protective effects of memantine against immobility. Memantine significantly inhibited the excessive glutamate production and improved impaired neurogenesis on first and seventh day after sepsis, accompanying with reducing proinflammatory cytokines production (tumor necrosis factor alpha (TNF- $\alpha$ ), interleukin (IL)-1beta (IL-1 $\beta$ ), and IL-10) and microglia activation in the brain of SAE. In addition, memantine treatment also reducing sepsis-induced brain blood barrier disruption via inhibiting the expression of metalloproteinase-9 (MMP-9). In conclusion, memantine exerted neuro-protective effects against cognitive and emotional defects, which might be considered as a promising therapy for SAE.



## 1. BACKGROUND

Sepsis-associated encephalopathy (SAE) is the most common complication of sepsis, which is characterized by mental confusion, anxiety, irritability, depression, decreased learning capacity and memory, as well as social communication, in the absence of the direct infection in central nervous system.<sup>1</sup> SAE contributed to the increased mortality in patients with sepsis, prolong hospitalization, as well as the reduced quality of life in survivors with sepsis, which loaded heavy economic burdens to the country and family.<sup>2</sup> However, there is still no established pharmacological therapy.

To date, the exact pathophysiology and pathogenesis of SAE are not clear. More and more evidence suggested that the pathophysiology of SAE was complex and multifactorial, combining intertwined or parallel processes, and was promoted by countless alterations and dysfunctions caused by sepsis, including peripheral inflammation, neuroinflammation, oxidative stress, mitochondrial dysfunction, reduced brain metabolism, imbalance or translocation of neurotransmitters (glutamate) and ions ( $\text{Ca}^{2+}$ ), neuronal apoptosis and autophagy as well as disruptions to the integrity of the blood-brain barrier (BBB).<sup>3–5</sup> It was well accepted that the level of glutamate in SAE brain was increased while the increased glutamate as the primary excitatory neurotransmitter contributed to the clinical

presentations of SAE, such as depression, anxiety and decreased learning and memory capacity.<sup>2</sup> Glutamate induced excitatory neurotoxic effects were mediated by NMDA (*N*-methyl-D-aspartate) receptor. Glutamate binding to NMDA receptors resulted in calcium overload via calcium influx, which triggered the activation of calpains and other proteases mediating cytoskeleton damage, paralleled by reactive oxygen species generation, mitochondrial dysfunction, and subsequent neuronal apoptosis.<sup>6</sup> In addition,  $\text{Ca}^{2+}$  influx rendered the inflammasome activation in response to infection.<sup>7</sup> These above progresses also contributed to the pathophysiology of SAE. More important, NMDA receptors antagonist could preferentially block glutamate induced neurotoxicity without interfering with NMDA receptor function needed for normal synaptic transmission and plasticity.<sup>6,8</sup> In addition, inhibiting NMDA receptor also attenuates LPS (lipopolysaccharide)

Received: August 22, 2023

Accepted: September 26, 2023

Published: October 16, 2023



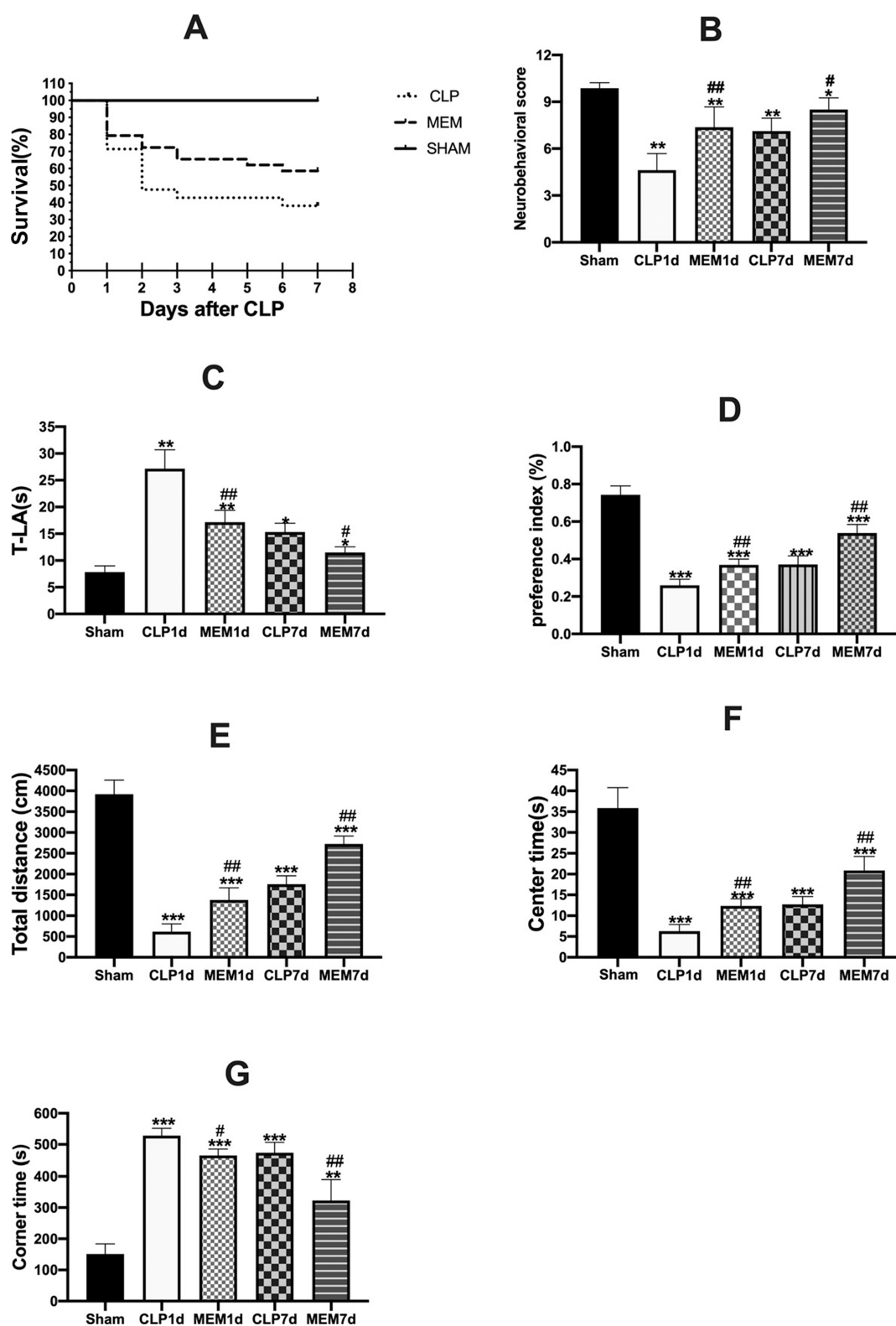


**Figure 1.** Memantine improved survival rate and ameliorated cognitive and emotional dysfunction of CLP-induced sepsis in mice. (A) Survival curve 8 of 21 mice of CLP group survived by day 7. Seventeen of 29 mice of memantine treatment survived by day 7. (B, C) Bar graphs showing statistical analysis of neurobehavioral scores (B) and T-LA (C). (D) The bar graph showing statistical analysis of the preference index in NORT. (E–G) The bar graphs showing statistical analysis of total distance (E), center time (F) and corner time (G) in OFT respectively. \* $p < 0.05$ , \*\* $p < 0.01$ , \*\*\* $p < 0.001$  vs sham group, # $p < 0.05$ , ## $p < 0.01$ , ### $p < 0.001$ , CLP (cecal ligation and puncture) group vs Memantine (MEM) group. Data are presented as mean  $\pm$  SEM. CLP 1d: CLP group on 1st day after surgery. CLP7d: CLP group on 7th day after surgery. MEM 1d: receiving memantine treatment of CLP group on 1st day after surgery. MEM7d: receiving memantine treatment of CLP group on 7th day after surgery.

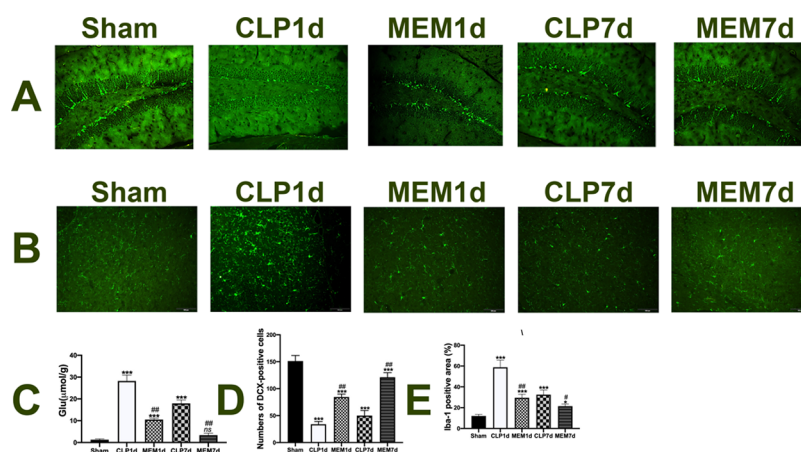


**Figure 2.** Memantine inhibited the level of glutamate as well as microglia activation and improved the impaired neurogenesis caused by CLP-induced sepsis in mice. (A, B) Representative immunofluorescence staining of DCX (A) in the hippocampus and Iba-1 (B) in the cortex. (C) Bar graph showing statistical analysis of the levels of glutamate in the brain. (D) The bar graph shows statistical analysis of the number of DCX-positive cells in the hippocampus. (E) The bar graphs showing statistical analysis of the area of Iba-1-positive cells in the cortex. \* $p < 0.05$ , \*\* $p < 0.01$ , \*\*\* $p < 0.001$  vs sham group, # $p < 0.05$ , ## $p < 0.01$ , ### $p < 0.001$ , CLP (cecal ligation and puncture) group vs Memantine (MEM) group. ns: no significance. Data are presented as mean  $\pm$  SEM. CLP 1d: CLP group on 1st day after surgery. CLP7d: CLP group on 7th day after surgery. MEM 1d: receiving memantine treatment of CLP group on 1st day after surgery. MEM7d: receiving memantine treatment of CLP group on 7th day after surgery

induced microglia inflammation *in vitro*<sup>9</sup> while activated microglia induced neuroinflammation was involved the process of SAE.<sup>1</sup> *In vitro* and *in vivo*, excess glutamate could enhance the permeability of BBB (blood brain barrier) via NMDA receptors.<sup>10</sup> NMDA receptor antagonist was found to reduce BBB permeability of experimental subarachnoid hemorrhage in the rat.<sup>11</sup> Thus, we speculated that NMDA receptor antagonist might exert neuroprotective effects on SAE.

Memantine as be the low-affinity, fast off-rate, voltage-dependent, and uncompetitive NMDA receptor antagonist has been approved to treat moderate to severe Alzheimer's disease (AD) by FDA (food and drug administration).<sup>12</sup> Now, there are more and more evidence for memantine to treat other different neuropsychiatric disorders, including chronic pain,<sup>13</sup> psychiatry symptoms (including anxiety and cognitive dysfunction) of Parkinson's disease,<sup>14</sup> and schizophrenia (depression)<sup>15</sup> by anti-inflammatory effects. In addition, more and more research has focused on other disease animal models involved infection. Memantine could block meningitic *Escherichia coli* K1 bacteria neuro-invasion in mice via inhibiting neuroinflammation.<sup>16</sup> In addition, memantine was also proved to ameliorate the disruption of BBB model *in vitro* via inhibiting the expression of cell adhesion molecules to prevent monocytes transmigration except for inhibiting inflammation.<sup>17</sup> Memantine was also confirmed to alleviate sepsis induced acute lung injury in mice via inhibiting macrophage pyroptosis<sup>7</sup> while pyroptosis was involved in SAE.<sup>18</sup> Memantine was confirmed to attenuate spatial learning and memory impairments, which were caused by chronic LPS-infusion into the fourth ventricle.<sup>19</sup> More importantly, memantine is a safe and well-tolerated drugs with minimal differences from placebo in adverse event rates.<sup>20</sup>

Based on the above aforementioned findings, we hypothesized that memantine might have neuroprotective effects on neurobehavioral dysfunction in a mouse model of SAE induced by cecal ligation and puncture (CLP). In addition, we also tried to explore possible mechanisms of memantine on SAE.

## 2. RESULTS

### 2.1. Memantine not only significantly improved survival rate but also significantly ameliorated neurobehavioral dysfunction of CLP-induced sepsis in mice.

As illustrated in Figure 1A, the survival curve showed that the survival rate of the MEM group was improved, compared to the CLP group. Throughout the 7-day study period, all of the sham group showed 100% survival. However, CLP group showed 38.1% survival (8 of 21 mice survived) on seventh day after sepsis induction while Memantine group showed 58.6% survival (17 of 29 mice survived) by seventh day after sepsis induction. More importantly, there was significant difference between MEM group and CLP group ( $p < 0.01$ ) in the survival rate.

Behavioral tests, including neurobehavioral score, pole test, OFT and NORT, were carried out on first day and seventh day after CLP surgery. We used the neurobehavioral score system to evaluate neurobehavioral defects caused by sepsis. Compared to the sham group, sepsis significantly decreased the neurobehavioral score on the first day and seventh day after surgery while memantine significantly improved the decreased neurobehavioral score caused by sepsis on the first and seventh day after surgery (Figure 1B). T-LA measured by pole test was used to reflect the locomotion activity of survivor mice. As illustrated in Figure 1C, T-LA in CLP group on the first day and seventh day after surgery were significantly prolonged while memantine significantly decreased the prolonged T-LA caused by sepsis on the both times. OFT was carried out to assess the locomotion and anxiety-like behavior. The data demonstrated that septic mice spent more time in the corner area (Figure 1F) and less time in the center area (Figure 1G) as well as exhibited significantly decreased total distance (Figure 1E) during the OFT, compared to the sham group. However, memantine significantly improved the defective display of septic mice in OFT (Figure 1E-G). NORT was performed to evaluate the ability of learning and memory of mice. As illustrated in Figure 1D, the preference index of septic mice was significantly decreased on the first and seventh day

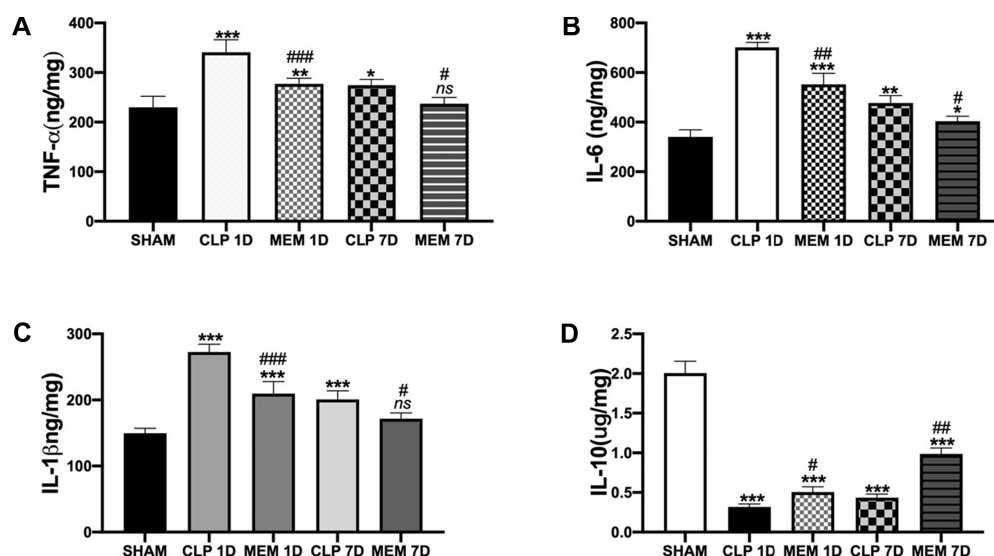


**Figure 3.** Memantine inhibited the expressions of proinflammatory cytokines and improved the expression of anti-inflammatory cytokine. (A–D) The bar graphs showing that statistical analysis of the levels of proinflammatory cytokines: TNF- $\alpha$  (A), IL-6 (B) and IL-1 $\beta$  (C) as well as the level of anti-inflammatory cytokine: IL-10 (D) measured by ELISA. Data was presented as mean  $\pm$  SEM \* $p$  < 0.05, \*\* $p$  < 0.01, \*\*\* $p$  < 0.001 vs sham group, # $p$  < 0.05, ## $p$  < 0.01, ### $p$  < 0.001, CLP (cecal ligation and puncture) group vs Memantine (MEM) group. *ns*: no significance. Data are presented as mean  $\pm$  SEM. CLP 1d: CLP group on 1st day after surgery. CLP7d: CLP group on 7th day after surgery. MEM 1d: receiving memantine treatment of CLP group on 1st day after surgery. MEM7d: receiving memantine treatment of CLP group on 7th day after surgery.

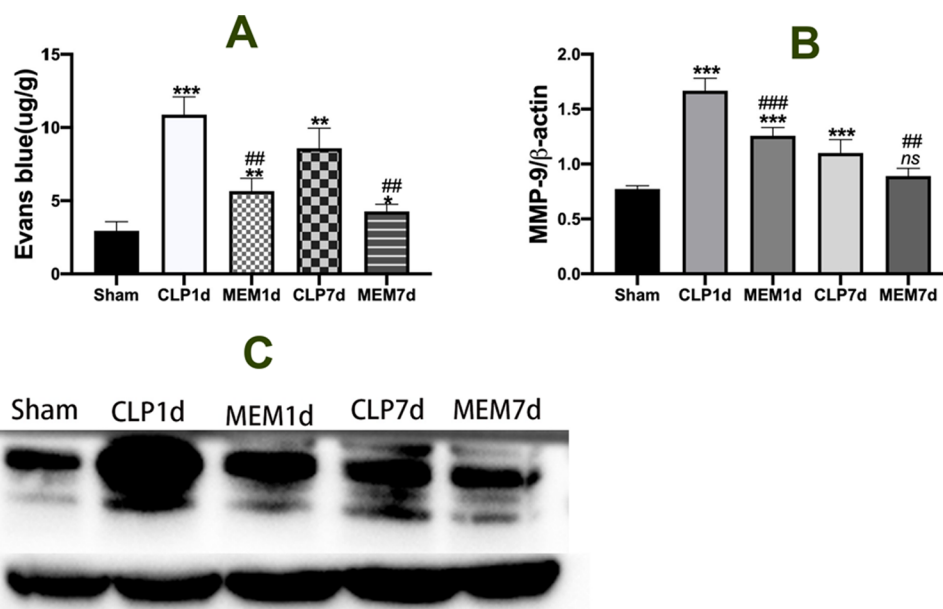


**Figure 4.** Memantine alleviated the disintegration of the BBB and inhibited the level of MMP-9 in the brain of CLP-induced septic mice. (A) The bar graph showing that statistical analysis of the permeability of BBB on different time was evaluated by Evans blue dye. (B) Quantitative statistical analysis of the relative MMP-9 expression in the brain on different times.  $\beta$ -actin was used as a loading control. (C) Representative Western blotting bands of MMP-9 in the SAE. \* $p$  < 0.05, \*\* $p$  < 0.01, \*\*\* $p$  < 0.001 vs sham group, # $p$  < 0.05, ## $p$  < 0.01, ### $p$  < 0.001, CLP (cecal ligation and puncture) group vs Memantine (MEM) group. *ns*: no significance. Data are presented as mean  $\pm$  SEM. CLP 1d: CLP group on 1st day after surgery. CLP7d: CLP group on 7th day after surgery. MEM 1d: receiving memantine treatment of CLP group on 1st day after surgery. MEM7d: receiving memantine treatment of CLP group on 7th day after surgery.

after surgery, while memantine significantly improved the decreased preference index of septic mice on both times.

Collectively, these results indicated that CLP-induced septic mice exhibited bradykinesia, cognitive dysfunction, and emotional disorder, while memantine treatment relieved these neurobehavioral deficits.

**2.2. Memantine not only significantly inhibited the level of glutamate in septic mice but also alleviated the**

**decreased neurogenesis caused by CLP-induced sepsis in mice.** To identify whether the effects of memantine on neurobehavioral deficits were related to the neurogenesis, brain sections were used to perform fluorescent immunohistochemical staining after completing the behavioral test. The results showed that the numbers of DCX-positive cells in dentate gyrus of the septic mice's hippocampus on the first and seventh day after surgery were significantly decreased comparing to the

sham group (Figure 2A and 2D). However, memantine treatment significantly improved the decreased the number of DCX-positive cells in dentate gyrus (Figure 2A and 2D). In addition, we also noticed that the pattern of DCX-positive cells in septic mice was loosen and disordered while the pattern of DCX-positive cells in the memantine group was relatively well-organized. To further define whether the level of glutamate contributes to the decreased neurogenesis, we measured the levels of glutamate in the brain by Glutamate Assay Kit. As illustrated in Figure 2C, the level of glutamate in septic mice was significantly increased on the first and seventh day after surgery while memantine significantly prevented the increased glutamate level of septic mice on the both times. However, we also noticed that there was no difference on the level of glutamate between the memantine treatment group and the sham group, although the level of glutamate in the memantine group was higher than that in the sham group (Figure 2C) on seventh day after surgery.

**2.3. Memantine significantly decreased the level of inflammatory cytokines as well as diminished microglia activation in the brain of septic mice.** To determine whether the imbalance of pro-inflammatory cytokines and anti-inflammatory cytokines contributes to neurobehavioral deficits, we measured the levels of cytokines in the brains. The results showed that sepsis significantly the levels of pro-inflammatory cytokines, including TNF- $\alpha$  (Figure 3A), IL-6 (Figure 3B) and IL-1 $\beta$  (Figure 3C) and significantly reduced the level of anti-inflammatory cytokine (IL-10) (Figure 3D) on the first and seventh day after surgery. However, memantine treatment significantly decreased the levels of pro-inflammatory cytokines, including TNF- $\alpha$  (Figure 3A), IL-6 (Figure 3B) and IL-1 $\beta$  (Figure 3C) and significantly reduced the level of anti-inflammatory cytokine (IL-10) (Figure 3D), induced by sepsis, on the first and seventh day after surgery. However, we also noticed that there was no difference on the levels of IL-1 $\beta$  (Figure 3C) and TNF- $\alpha$  (Figure 3A) between the memantine treatment group on seventh day after surgery and the sham group (Figure 4B). To further confirm the effect of microglia on the inflammatory response of SAE, fluorescent immunohistochemical staining of Iba-1 was performed to observe the numbers and morphology of microglia cells in the brain. As illustrated in Figure 2B, Iba1-positive cells in septic mice showed an enlarged cell body with shorter, shortened processes, which were consistent with the amoeboid morphology of activated microglia. However, Iba-1 positive cells in sham group showed a thin cell body with fine and long processes, consistent with the ramified morphology of resting microglia. In addition, the numbers of Iba1-positive cells in septic mice were significantly increased on the first and seventh day after surgery, comparing to the sham group (Figure 2E). More importantly, we found that memantine treatment significantly reduced the number of activated amoeboid morphology microglia cells on the first and seventh day after surgery (Figure 2B,E).

**2.4. Memantine significantly alleviated the disintegration of the BBB and inhibited the level of MMP-9 in the brain of CLP-induced septic mice.** To further whether the permeability of BBB contributes to the neurobehavioral deficits of septic mice, an Evans blue dye test was performed. As illustrated in Figure 4A, the levels of Evans blue dye in septic mice on the first and seventh day after surgery were significantly higher than those in sham group while memantine treatment significantly decreased the enhanced levels of Evans

blue dye in septic mice on both times. The data indicated that memantine treatment significantly alleviated the increased permeability of the BBB caused by sepsis. To further confirm the permeability of BBB, we measured the level of MMP-9 via Western Blot. The results suggested that sepsis significantly enhanced the expressions of MMP-9 in the brain on the first and seventh day after surgery while memantine treatment significantly alleviated the increased expressions of MMP-9 in septic mice on both times (Figure 4B,C). However, we also noticed that there was no difference on the level of MMP-9 between the memantine treatment group on the seventh day after surgery and the sham group (Figure 4B).

### 3. DISCUSSION

Memantine attracts more and more attention because of the effects on the cognitive and emotional dysfunction of some disorders, while cognitive and emotional dysfunctions were also the manifestations of SAE. To our limited acknowledgment, we for the first time demonstrated that memantine not only improved the neurobehavioral dysfunction, impaired endoneurogenesis as well as the integrity of BBB, but also decreased the mortality, excessive production of pro-inflammatory cytokines and glutamate, as well as activation of microglia in the brain of SAE. This finding suggested a novel application of memantine in SAE, which is currently lacking effective therapy.

CLP is not only a gold standard model to mimic clinical sepsis and but also the ideal animal model of SAE, which was able to cause short-term and long-term behavioral and cognitive impairment.<sup>21</sup> Thus, we selected CLP as the animal model of SAE for further researches. After modeling with CLP, we measured neurobehavioral test scores to analyze whether the SAE rat model was successfully established. Consistent with previous research,<sup>22</sup> SAE models caused by CLP were successfully established while memantine treatment not only significantly decreased the mortality of sepsis but also significantly improved the neurobehavioral test scores (Figure 1A,B). It indicated that memantine treatment attenuated the severity of SAE. The OFT is a widely used to evaluate emotion in animals. Mice typically preferred not to be center and tended to close to the wall/corner since it came to the new environment, which reflected the anxiety. The total distance in OFT reflected the immobility and locomotion activity of mice.<sup>21</sup> In addition, T-LA also reflected the locomotion of mice. The NORT was a relatively fast and efficient means for testing learning and memory in mice and required less time than commonly used tests, such as Morris water maze or Barnes maze.<sup>23</sup> Preference index in NORT reflected the ability to learn and memory in mice. Our results indicated that CLP resulted in the cognitive dysfunction, impaired locomotion, anxiety, and prolonged immobility (Figure 1C-G) on the first and seventh day after surgery, which were consistent with the clinical presentations of SAE.<sup>2</sup> These results further confirmed that SAE models caused by CLP were successfully established. The oral bioavailability of memantine is almost 100%, following oral administration.<sup>13</sup> Thus, we selected intragastric administration as a means of giving drugs. Consistent with the effects of memantine on the cognitive and emotion in other diseases,<sup>12,14</sup> our results also suggested that memantine treatment improved the cognitive dysfunction, impaired locomotion, anxiety, and prolonged immobility caused by sepsis (Figure 1C-G) on the first and seventh day after surgery.

This reminded us that memantine exerted neuroprotective effects on SAE.

Growing evidence suggested that excessive glutamate production and impaired neurogenesis in hippocampus contributed to the neurobehavioral dysfunctions, such as impaired cognitive and emotion of SAE.<sup>2,3,24</sup> In agreement with previous researches,<sup>3,6,24,25</sup> our results also demonstrated that CLP-induced SAE also exhibited the excessive glutamate level and impaired neurogenesis in the hippocampus (Figure 2A,C,D). And, memantine treatment improved the neurogenesis (Figure 2A) and decreased the level of glutamate (Figure 2C) in the brain. It has been confirmed that excessive glutamate could result in neuron apoptosis or impaired neurogenesis via binding to NMDA receptors mediating  $\text{Ca}^{2+}$  overload.<sup>6,26</sup> Therefore, we deduced that impaired neurogenesis in SAE was at least partly caused by excessive glutamate production resulting from sepsis, while memantine might improve neurogenesis via inhibiting excessive glutamate as well as inhibiting  $\text{Ca}^{2+}$  overload through binding to NMDA receptors.

Neuroinflammation and destruction of BBB also played an important role in the cognitive impairment of SAE.<sup>2,5</sup> Consistent with above findings, our results demonstrated that destruction of BBB as well as proinflammatory reactions were significantly activated, which contributed to the cognitive impairment of SAE. Increasing evidence suggested that excessive glutamate production increased the permeability of BBB via NMDA receptor dependent mechanism.<sup>10</sup> More importantly, NMDA receptor antagonists improved the dis-integrity of BBB in animal models of brain injury, such as subarachnoid hemorrhage,<sup>11</sup> ischemic stroke<sup>27</sup> and epilepsy.<sup>10</sup> In addition, IL-1 $\beta$ , IL-6 and TNF- $\alpha$  in the brain known as the pro-inflammatory cytokines also contributed to the dis-integrity of BBB in SAE except for mediating the initial response of the innate immune system to injury or infection during SAE.<sup>5</sup> In addition, excessive glutamate also returned to result in neuroinflammatory reactions in the brain.<sup>28</sup> Thus, the results indicated that memantine exhibited neuroprotective effects on SAE through direct and indirect effects. Consistent with previous researches,<sup>10,19</sup> direct effects of memantine on SAE included improving the dis-integrity of BBB and inhibiting proinflammatory reactions. And the indirect effects of memantine on SAE preferred that integrity of BBB and balance between proinflammation and anti-inflammation were regained mediated decreased glutamate production. Matrix metalloproteinases (MMPs) as the most important ECM (extra-cellular matrix)-degrading enzyme in vivo, were a family of zinc-dependent endopeptidases which degrade the basement membranes and extracellular matrix of surrounding cells<sup>29</sup> and were the major contributor to BBB disruption.<sup>30</sup> Our results indicated that memantine improved the permeability by inhibiting MMP-9 expression.

Microglia as the primary immune cells in the brain exerted two phenotypes. Sepsis could make microglia shift from resting phenotype to proinflammatory amoeboid morphology, which released those above inflammatory cytokines.<sup>1</sup> More importantly, activated microglia secreted those pro-inflammatory cytokines, including IL-1 $\beta$ , IL-6 and TNF- $\alpha$ . Microglia mediated neuroinflammation or neuroinflammation played an important role in the development of cognitive dysfunction after sepsis.<sup>22</sup> Inhibiting microglia activation or neuroinflammation was able to improve cognitive dysfunction.<sup>31</sup> Our results suggested that sepsis induced the resting microglia

to active microglia at the early stage (Figure 2B), accompanied by increased proinflammatory cytokine production (TNF- $\alpha$ , IL-6 and IL-1 $\beta$ , Figure 3A-C) and decreased anti-inflammatory cytokine (IL-10, Figure 3D). The results provided evidence for us that memantine alleviated cognitive deficits via inhibiting microglia activation or neuroinflammation. In the current preliminary study, we did not further explore whether memantine exerted neuroprotective effects mediating  $\text{Ca}^{2+}$  influx. Thus, we guaranteed further research to explore the effects of the inhibiting  $\text{Ca}^{2+}$  influx mediating NMDA receptors antagonist on SAE

## 4. CONCLUSION

In summary, our study provided valuable data that memantine treatment not only significantly improved the survival rate after sepsis but also significantly improved cognitive and emotional dysfunction, accompanied by reducing the level of glutamate, microglia activation, proinflammatory reaction, and improving neurogenesis and the dis-integrity of BBB. These data suggested that memantine might be considered as a promising therapy for SAE.

## 5. MATERIALS AND METHODS

**5.1. Animals.** Male C57BL/6 mice (n = 160) aged 10–12week enrolled in this study were obtained from Jinan Pengyue laboratory animal breeding co. ltd. The animals were housed under standard laboratory conditions and maintained in temperature and humidity controlled rooms on a 12h/12h light/dark cycle. All the animal protocols and procedures described in this study were approved and in accordance with the guidelines of the Experimental Animal Ethical Committee of Shandong Province Hospital affiliated with Shandong First Medical University. All of the animals had acclimated to the environment for at least 7 days prior to experiments. All efforts were taken to minimize the number of animals and overall suffering to the animals.

**5.2. Animal model preparation, grouping and treatment.** Mice were randomly divided into 3 groups: MEM (memantine) group referring to the cecal ligation and puncture (CLP) group receiving MEM, CLP group referring to the CLP model group receiving the same volume of saline, and Sham group receiving saline. Mice were subjected to cecal ligation and puncture (CLP) model to induce sepsis described previously with modifications.<sup>32</sup> In brief, after mice were intraperitoneally anesthetized with pentobarbital sodium in saline (50 mg/kg, Sigma, St Louise, MO, USA), a longitudinal skin midline incision was performed in the lower abdomen. The cecum was isolated carefully and ligated with 4.0 silk below the ileocecal junction, approximately 1.2 cm from the distal end. The cecum was punctured on the antimesenteric side with a sterile 21-gauge needle and was gently squeezed to extrude the fecal contents into the peritoneal cavity. Then, the cecum was gently returned to the peritoneal cavity, and the abdomen is sutured with 3.0 silk. All mice were subcutaneously administered with prewarm normal saline 50 mL/kg immediately after surgery as fluid resuscitation. The entire procedure was controlled in approximately 10 min for each animal. After surgery, the body temperature was maintained at  $37 \pm 0.5$  °C with a thermostatically controlled infrared lamp during the procedure. In the sham group, mice received the operation as described above, but they were neither ligated nor punctured. Above these three groups were also divided into

two subgroups at the first and seventh day after surgery. Memantine (MEM, Sigma, St Louis, MO, USA) was dissolved in PBS (phosphate buffered solution) with a final concentration of 10 mg/mL. All the mice began to receive intragastric administration of memantine (20 mg/kg) or equal volume of PBS once a day for 2 consecutive days before surgery until being sacrificed. All of the mice had free access to food and water during the whole experiment. The 7 day survival rates were recorded by the blind examiner for the group assignments.

**5.3. Neurobehavioral tests.** The blind examiner to the group assignments performed all of the neurobehavioral tests, which included neurobehavioral score, pole test, open field test (OFT) and novel object recognition test (NORT) on the first day and seventh day after surgery. Because there was no statistical difference in neurobehavioral analysis between the first and seventh day of the sham groups (the data did not show), we just chose the seventh day after sham operation as the sham group.

**5.3.1. Neurobehavioral score.** Neurobehavior score was used to evaluate neurobehavior change according to the previous report.<sup>33</sup> The score system consisted of five parts, which included the corneal reflex, the auricle reflex, the righting reflex, the tail-flick reflex, and the avoid reflex. Corneal reflex referred to the mouse blinking its eye or shaking its head after the cornea of the mouse was contacted gently with a cotton swab. Auricle reflex referred to strong head rotation caused by touching the mouse's plane. Righting reflex refers to the ability to turn into the prone position and place both feet on the floor after the mouse is placed in the supine position. Tail-flick reflex and avoid reflex refer to the escaping ability after the mouse's tail was briefly stimulated. If the mouse had a normal reflex, this was scored as 2 points, while hyperreflexia (lack of reflex in 10 s) scored 1 point and areflexia scored 1 point. The total scores of these five tests were added up to 10 points. A lower score was correlated with the worst neurobehavior.

**5.3.2. Pole test.** The pole test was performed to evaluate bradykinesia of SAE model according to previously described.<sup>34</sup> Briefly, mice were placed on the top of the wooden pole (10 mm in diameter and 60 cm in height with a rough surface). The time for the mice to arrive at the floor was recorded as locomotor activity time (T-LA). Each trial duration was 30s. If the mice did not climb down and place four feet on the floor in 30s, they were guided. And the T-LA was recorded as 30s. The mice were pretrained before test. Each mouse was tested three times, and the average of 3 trials were calculated for further statistical analysis. A higher score was correlated with severe movement impairment.

**5.3.3. Open field test (OFT).** The open field test was conducted to test the level of anxiety through locomotor activities according to previously described with modifications.<sup>35</sup> In brief, the apparatus was a square light-gray polyvinyl chloride (PVC) box of 50 × 50 × 50 cm, and the ground of the open field was divided into 9 equal squares by black lines. The mice were gently placed in the center quadrant. Habituation to an open field was performed in the same PVC box for 5 min one h before test. The box was cleaned with 70% ethanol and a paper towel before proceeding to the next test animal. The test duration was 10 min. The total distance and time spent in the center and corner were recorded.

**5.3.4. New object recognition test (NORT).** The new object recognition test was performed according to previously

described.<sup>23</sup> The apparatus was a square box (40 × 40 × 40 cm) made of white and nonporous plastic. The whole procedure consisted of 3 phases, including habituation phase, familiarization phase, and discrimination phase. The habituation phase was carried out before the surgery. Each mouse was placed in the center of the square open box and allowed to explore freely for 10 min per day in the absence of objects for three consecutive days. Then the animals entered the familiarization phase. In this phase, each mouse was allowed to explore the square open box with two identical objects (A1 and A2) located in opposite and equidistant positions for 10 min. After a three h retention interval, the mouse returned to the open field, with one of the familiar objects (A1) replaced by a novel object (A3). For the discrimination phase, each mouse was allowed to explore for 10 min, and the time for exploring each object was recorded. Mice touching an object or facing an object within 2 cm around the object were taken as a measure of object exploration behavior. To eliminate possible olfactory cues, the objects and field were cleaned with 75% ethanol and a paper towel between each trial. The preference index was determined as [time spent in exploring the novel object (A3)/time spent in exploring the two objects (A2 and A3)] × 100%.

**5.4. Assessment of blood brain barrier (BBB) integrity/permeability.** After performing neurobehavioral tests, some of the mice (n = 4 every group) were sacrificed for assessment of BBB integrity. The level of BBB integrity was measured by Evans blue extravasation method according to previously described with modification.<sup>36</sup> In brief, Evans blue dye (2% in saline) was administrated at 3 mL/kg via tail vein. The mice were perfused with ice saline to wash residual dye from the blood vessel at 2h after injection until the fluid from the right atrium was colorless. Then the brain tissue was immediately removed on ice, collected, weighed, and manually homogenized in 1 mL of 50% trichloroacetic acid. After the homogenates were centrifuged at 10,000 rpm/min, the supernatant were diluted 4-fold with ethanol. The fluorescence absorbance was measured at 620/680 nm using a microplate reader (Bio-Rad, Philadelphia, PA, USA). The content of the Evans blue dye was calibrated with a standard curve of Evans blue in ethanol. Each Evans blue dye standard and sample were run in duplicate. Data are expressed as micrograms per milligram of brain weight.

**5.5. Fluorescent immunohistochemical staining.** At the end of neurobehavioral tests, mice were sacrificed for transcardial perfusion with ice saline followed by 4% paraformaldehyde (PFA) in PBS. Then, the brains were removed and fixed in PFA at 4 °C overnight, respectively, dehydrated in 30% and 20% sucrose solution at 4 °C overnight. The brains were frozen in Tissue-Tek embedding compound (Sakura Finetek, Japan) and cryosectioned into 10- $\mu$ m-thick slices on a cryostat (Leica CM1850, Germany). The slices of the brains were used for further immunohistochemical staining. Ten serial sections at the level of the hippocampus or frontal cortex with an interval of 50  $\mu$ m were obtained from each mouse. The sections were washed in PBS, blocked in 0.4% Triton X-100 (Sigma) in PBS for 15 min, then washed twice in PBS for 5 min, and 5% goat serum in PBS (Jackson ImmunoResearch Lab) for 1h followed by incubation with rabbit anti-Iba-1 (1:500, Wako, Japan) and rabbit antidoublecortin (DCX, 1:2000, Abcam) antibodies overnight at 4 °C. After washing twice in PBS, sections were incubated with secondary antibody FITC-conjugated goat antirabbit IgG (1:200 Jackson Immu-

noResearch Lab) for 2 h in the dark at room temperature. Finally, sections were mounted with the medium containing DAPI for fluorescence (Vector Laboratories) and viewed by fluorescence microscopy (Olympus, Japan). The number of DCX-positive cells was counted at 200 $\times$  magnification. Then the data from bilateral hippocampus were averaged, expressed as the mean  $\pm$  SEM. The percent of Iba-1 positive cells occupied the whole slice was counted at 200 $\times$  magnification and autoanalyzed by the software IPP 6.0. Then the data from the bilateral cortex were averaged, expressed as the mean  $\pm$  SEM.

**5.6. Cytokine Assessment.** At the end of neurobehavioral tests, mice were sacrificed and the fresh brain tissue was quickly isolated and kept at  $-80^{\circ}\text{C}$  for Enzyme-Linked Immunosorbent Assay (ELISA), Western Blot as well as glutamate assay. ELISA kits for cytokine in brains including tumor necrosis factor alpha (TNF- $\alpha$ ), interleukin (IL)-1beta (IL- $\beta$ ), and IL-10 were purchased from Boster (Wuhan, China). In brief, the brain tissue were minced and homogenized in a 1:10 dilution ice NP40 lysis with protease inhibitor complex for 20 min. Then the complete homogenate were centrifuged at 12,000 rpm for 30 min at  $4^{\circ}\text{C}$  and the supernatant was collected for further measurement of above those cytokines according to the manufacturer's instructions. Absorbance was recorded at 450 nm using microplate reader (Biorad, USA). Each standard and experimental sample were run in duplicate.

**5.7. Western Blot.** After performing neurobehavioral tests, some of the mice ( $n = 5$  every group) were sacrificed and fresh brain tissue was rapidly isolated on ice for further Western Blot analysis. The tissue was homogenized in ice-cold RIPA lysis buffer (150 mM NaCl, 50 mM Tris at pH 7.4, 0.5% deoxycholic acid, 0.1% SDS, 1% Triton X-100, 2.5 mM EDTA, and protease inhibitors) (Beyotime, China). Each homogenate was centrifuged at 12,000 rpm for 30 min at  $4^{\circ}\text{C}$ . The supernatant was collected, and protein concentration was measured using a BCA protein assay kit (Beyotime, China). Proteins were separated on 10% SDS polyacrylamide gels according to the molecular weight of the detection proteins and transferred onto PVDF membranes by electrophoresis. The membranes were blocked with 5% non-fat milk in TBST (TBS containing 0.1% Tween-20) for 1h and incubated with rabbit anti-MMP-9 (matrix metalloproteinase-9) (1:500, Abgent) and mouse anti- $\beta$ -actin (1:1000, Santa Cruz) primary antibodies overnight at  $4^{\circ}\text{C}$ , followed by staining with goat antirabbit and antimouse secondary antibodies conjugated to horseradish-peroxidase (HRP, Beyotime, China) for 1 h at room temperature. Finally, reactions were detected by a chemiluminescence assay. Blots were analyzed three times for every set of experiments. Bands were normalized to  $\beta$ -actin levels and the density of the band was measured using ImageJ analysis software (NIH, Bethesda, MD, USA). Data were averaged, expressed as the mean  $\pm$  SEM, and compared between two groups.

**5.8. Glutamate analysis.** Glutamate concentration was measured with a Glutamate Assay Kit (Solarbio, China). After performing neurobehavioral tests, 0.1 g of the fresh brain tissue was homogenized in 1 mL of ice-cold Assay buffer and then centrifuged at 10,000 rpm for 10 min at room temperature (RT). Then, the supernatant was isolated and kept in a new centrifuge tube for further detection. The detailed assay method was performed according to the manufacturer's instructions. Absorbance was recorded at 340 nm using

colorimetric readout (Biorad, USA). Each glutamate standard and sample were run in duplicate.

**5.9. Statistical analysis.** Statistical analysis was performed using GraphPad Prism 9 (GraphPad Software, La Jolla, CA). Data were expressed as means  $\pm$  SEM. One-way ANOVAs followed by post hoc Tukey multiple comparisons was used to analyze data for all experiments except for survival rate. The survival rate was estimated by the Kaplan–Meier method. Significance was set at  $P < 0.05$ .

## AUTHOR INFORMATION

### Corresponding Author

HongNa Yang – Department of Critical-Care Medicine, Shandong Provincial Hospital, Shandong University, Jinan 250021, China; Department of Critical-Care Medicine, Shandong Provincial Hospital Affiliated to Shandong First Medical University, Shandong First Medical University, Jinan 250021, China; [orcid.org/0000-0001-7573-5325](https://orcid.org/0000-0001-7573-5325); Email: [7216263@163.com](mailto:7216263@163.com)

### Authors

XiaoYu Zheng – Department of Critical-Care Medicine, Shandong Provincial Hospital, Shandong University, Jinan 250021, China

WenYu Li – Department of Critical-Care Medicine, Shandong Provincial Hospital Affiliated to Shandong First Medical University, Shandong First Medical University, Jinan 250021, China

Qian Xiang – Department of Critical-Care Medicine, Shandong Provincial Hospital, Shandong University, Jinan 250021, China

YanXue Wang – Department of Critical-Care Medicine, Shandong Provincial Hospital Affiliated to Shandong First Medical University, Shandong First Medical University, Jinan 250021, China

TingYu Qu – The Psychiatric Institute, Department of Psychiatry, College of Medicine, University of Illinois at Chicago, Chicago, Illinois 60612, United States

Wei Fang – Department of Critical-Care Medicine, Shandong Provincial Hospital Affiliated to Shandong First Medical University, Shandong First Medical University, Jinan 250021, China

Complete contact information is available at:  
<https://pubs.acs.org/10.1021/acsomega.3c06250>

### Author Contributions

#XiaoYu Zheng and WenYu Li contributed equally to this paper and are considered co-first authors. Hongna Yang designed the experiment and wrote the manuscript. Xiaoyu Zheng and Wenyu Li performed the neurobehavioral tests and glutamate analysis. Yanxue Wang performed Evans blue assess, Western Blot, Elisa and Fluorescent immunohistochemical staining. Tingyu Qu and Wei Fang contributed to study design, analysis, and interpretation. All authors read and approved the final manuscript. XiaoYu Zheng and WenYu Li contributed equally to this paper.

### Notes

The authors declare no competing financial interest.

## ACKNOWLEDGMENTS

This study was supported by grants from Natural Science Foundation of China (No. 81701057) to HongNa Yang.

## REFERENCES

- (1) Yan, X.; Yang, K.; Xiao, Q.; Hou, R.; Pan, X.; Zhu, X. Central role of microglia in sepsis-associated encephalopathy: From mechanism to therapy. *Front Immunol* **2022**, *13*, No. 929316.
- (2) Zhao, L.; Gao, Y.; Guo, S.; Lu, X.; Yu, S.; Ge, Z. Z.; Zhu, H. D.; Li, Y. Sepsis-Associated Encephalopathy: Insight into Injury and Pathogenesis. *CNS Neurol Disord Drug Targets* **2021**, *20* (2), 112–124.
- (3) Catarina, A. V.; Branchini, G.; Bettoni, L.; De Oliveira, J. R.; Nunes, F. B. Sepsis-Associated Encephalopathy: from Pathophysiology to Progress in Experimental Studies. *Mol. Neurobiol* **2021**, *58* (6), 2770–2779.
- (4) Zhou, R. X.; Li, Y. Y.; Qu, Y.; Huang, Q.; Sun, X. M.; Mu, D. Z.; Li, X. H. Regulation of hippocampal neuronal apoptosis and autophagy in mice with sepsis-associated encephalopathy by immunity-related GTPase M1. *CNS Neurosci Ther* **2020**, *26* (2), 177–188.
- (5) Ren, C.; Yao, R. Q.; Zhang, H.; Feng, Y. W.; Yao, Y. M. Sepsis-associated encephalopathy: a vicious cycle of immunosuppression. *J. Neuroinflammation* **2020**, *17* (1), 14.
- (6) Simões, A. P.; Silva, C. G.; Marques, J. M.; Pochmann, D.; Porciuncula, L. O.; Ferreira, S.; Oses, J. P.; Beleza, R. O.; Real, J. I.; Kofalvi, A.; Bahr, B. A.; Lerma, J.; Cunha, R. A.; Rodrigues, R. J. Glutamate-induced and NMDA receptor-mediated neurodegeneration entails P2Y1 receptor activation. *Cell Death Dis* **2018**, *9* (3), 297.
- (7) Ding, H.; Yang, J.; Chen, L.; Li, Y.; Jiang, G.; Fan, J. Memantine Alleviates Acute Lung Injury Via Inhibiting Macrophage Pyroptosis. *Shock* **2021**, *56* (6), 1040–1048.
- (8) Vyklicky, V.; Korinek, M.; Smejkalova, T.; Balik, A.; Krausova, B.; Kaniakova, M.; Lichnerova, K.; Cerny, J.; Krusek, J.; Dittert, I.; Horak, M.; Vyklicky, L. Structure, function, and pharmacology of NMDA receptor channels. *Physiol Res* **2014**, *63*, S191–S203.
- (9) Wu, Q.; Zhao, Y.; Chen, X.; Zhu, M.; Miao, C. Propofol attenuates BV2 microglia inflammation via NMDA receptor inhibition. *Can. J. Physiol. Pharmacol.* **2018**, *96* (3), 241–248.
- (10) Vazana, U.; Veksler, R.; Pell, G. S.; Prager, O.; Fassler, M.; Chassidim, Y.; Roth, Y.; Shahar, H.; Zangen, A.; Raccach, R.; Onesti, E.; Ceccanti, M.; Colonnese, C.; Santoro, A.; Salvati, M.; D'Elia, A.; Nucciarelli, V.; Inghilleri, M.; Friedman, A. Glutamate-Mediated Blood-Brain Barrier Opening: Implications for Neuroprotection and Drug Delivery. *J. Neurosci.* **2016**, *36* (29), 7727–39.
- (11) Germano, A.; Caffo, M.; Angileri, F. F.; Arcadi, F.; Newcomb-Fernandez, J.; Caruso, G.; Meli, F.; Pineda, J. A.; Lewis, S. B.; Wang, K. K.; Bramanti, P.; Costa, C.; Hayes, R. L. NMDA receptor antagonist felbamate reduces behavioral deficits and blood-brain barrier permeability changes after experimental subarachnoid hemorrhage in the rat. *J. Neurotrauma* **2007**, *24* (4), 732–44.
- (12) Atri, A. The Alzheimer's Disease Clinical Spectrum: Diagnosis and Management. *Med. Clin North Am.* **2019**, *103* (2), 263–293.
- (13) Kreutzwiser, D.; Tawfic, Q. A. Expanding Role of NMDA Receptor Antagonists in the Management of Pain. *CNS Drugs* **2019**, *33* (4), 347–374.
- (14) Vanle, B.; Olcott, W.; Jimenez, J.; Bashmi, L.; Danovitch, I.; IsHak, W. W. NMDA antagonists for treating the non-motor symptoms in Parkinson's disease. *Transl Psychiatry* **2018**, *8* (1), 117.
- (15) Cioffi, C. L. Modulation of NMDA receptor function as a treatment for schizophrenia. *Bioorg. Med. Chem. Lett.* **2013**, *23* (18), 5034–44.
- (16) Yu, J. Y.; Zhang, B.; Peng, L.; Wu, C. H.; Cao, H.; Zhong, J. F.; Hoffman, J.; Huang, S. H. Repositioning of Memantine as a Potential Novel Therapeutic Agent against Meningitic E. coli-Induced Pathogenicities through Disease-Associated Alpha7 Cholinergic Pathway and RNA Sequencing-Based Transcriptome Analysis of Host Inflammatory Responses. *PLoS One* **2015**, *10* (5), No. e0121911.
- (17) Wang, F.; Zou, Z.; Gong, Y.; Yuan, D.; Chen, X.; Sun, T. Regulation of Human Brain Microvascular Endothelial Cell Adhesion and Barrier Functions by Memantine. *J. Mol. Neurosci* **2017**, *62* (1), 123–129.
- (18) Xu, X. E.; Liu, L.; Wang, Y. C.; Wang, C. T.; Zheng, Q.; Liu, Q. X.; Li, Z. F.; Bai, X. J.; Liu, X. H. Caspase-1 inhibitor exerts brain-protective effects against sepsis-associated encephalopathy and cognitive impairments in a mouse model of sepsis. *Brain Behav Immun* **2019**, *80*, 859–870.
- (19) Rosi, S.; Vazdarjanova, A.; Ramirez-Amaya, V.; Worley, P. F.; Barnes, C. A.; Wenk, G. L. Memantine protects against LPS-induced neuroinflammation, restores behaviorally-induced gene expression and spatial learning in the rat. *Neuroscience* **2006**, *142* (4), 1303–15.
- (20) Kavirajan, H. Memantine: a comprehensive review of safety and efficacy. *Expert Opin Drug Saf* **2009**, *8* (1), 89–109.
- (21) Savi, F. F.; de Oliveira, A.; de Medeiros, G. F.; Bozza, F. A.; Michels, M.; Sharshar, T.; Dal-Pizzol, F.; Ritter, C. What animal models can tell us about long-term cognitive dysfunction following sepsis: A systematic review. *Neurosci Biobehav Rev.* **2021**, *124*, 386–404.
- (22) Zhou, R.; Sun, X.; Li, Y.; Huang, Q.; Qu, Y.; Mu, D.; Li, X. Low-dose Dexamethasone Increases Autophagy in Cerebral Cortical Neurons of Juvenile Rats with Sepsis Associated Encephalopathy. *Neuroscience* **2019**, *419*, 83–99.
- (23) Lueptow, L. M., Novel Object Recognition Test for the Investigation of Learning and Memory in Mice. *J. Vis Exp* **2017**, (. DOI: 10.3791/55718
- (24) Bluemel, P.; Wickel, J.; Grunewald, B.; Ceanga, M.; Keiner, S.; Witte, O. W.; Redecker, C.; Geis, C.; Kunze, A. Sepsis promotes gliogenesis and depletes the pool of radial glia like stem cells in the hippocampus. *Exp. Neurol.* **2021**, *338*, No. 113591.
- (25) Shen, Y.; Jing, L.; Zhang, Y.; Bao, H.; Vohra, A.; Si, Y.; Pan, C.; Xing, Y. CXCR5 Knockdown Attenuates Hippocampal Neurogenesis Deficits and Cognitive Impairment in a Mouse Model of Sepsis-associated Encephalopathy. *Neuroscience* **2020**, *433*, 212–220.
- (26) Rubio-Casillas, A.; Fernandez-Guasti, A. The dose makes the poison: from glutamate-mediated neurogenesis to neuronal atrophy and depression. *Rev. Neurosci* **2016**, *27* (6), 599–622.
- (27) Sifat, A. E.; Vaidya, B.; Abbruscato, T. J. Blood-Brain Barrier Protection as a Therapeutic Strategy for Acute Ischemic Stroke. *AAPS J.* **2017**, *19* (4), 957–972.
- (28) Shen, Z.; Xiang, M.; Chen, C.; Ding, F.; Wang, Y.; Shang, C.; Xin, L.; Zhang, Y.; Cui, X. Glutamate excitotoxicity: Potential therapeutic target for ischemic stroke. *Biomed Pharmacother* **2022**, *151*, No. 113125.
- (29) Visse, R.; Nagase, H. Matrix metalloproteinases and tissue inhibitors of metalloproteinases: structure, function, and biochemistry. *Circ. Res.* **2003**, *92* (8), 827–39.
- (30) Takata, F.; Dohgu, S.; Matsumoto, J.; Takahashi, H.; Machida, T.; Wakigawa, T.; Harada, E.; Miyaji, H.; Koga, M.; Nishioku, T.; Yamauchi, A.; Kataoka, Y. Brain pericytes among cells constituting the blood-brain barrier are highly sensitive to tumor necrosis factor-alpha, releasing matrix metalloproteinase-9 and migrating in vitro. *J. Neuroinflammation* **2011**, *8*, 106.
- (31) Mei, B.; Li, J.; Zuo, Z. Dexmedetomidine attenuates sepsis-associated inflammation and encephalopathy via central alpha2A adrenoceptor. *Brain Behav Immun* **2021**, *91*, 296–314.
- (32) Rittirsch, D.; Huber-Lang, M. S.; Flierl, M. A.; Ward, P. A. Immunodesign of experimental sepsis by cecal ligation and puncture. *Nat. Protoc* **2009**, *4* (1), 31–6.
- (33) Bi, W.; Lan, X.; Zhang, J.; Xiao, S.; Cheng, X.; Wang, H.; Lu, D.; Zhu, L. USP8 ameliorates cognitive and motor impairments via microglial inhibition in a mouse model of sepsis-associated encephalopathy. *Brain Res.* **2019**, *1719*, 40–48.
- (34) Park, G.; Park, Y. J.; Yang, H. O.; Oh, M. S. Ropinirole protects against 1-methyl-4-phenyl-1, 2, 3, 6-tetrahydropyridine (MPTP)-induced neurotoxicity in mice via anti-apoptotic mechanism. *Pharmacol., Biochem. Behav.* **2013**, *104*, 163–8.
- (35) Kraeuter, A.-K.; Guest, P. C.; Sarnyai, Z. The Open Field Test for Measuring Locomotor Activity and Anxiety-Like Behavior. In *Pre-Clinical Models*, 2019; pp 99–103.

(36) Goldim, M. P. S.; Della Giustina, A.; Petronilho, F. Using Evans Blue Dye to Determine Blood-Brain Barrier Integrity in Rodents. *Curr. Protoc Immunol* **2019**, *126* (1), No. e83.